



# Assessment of solar drying of Brazilian pulp mill primary sludge

Lindomar Matias Gonçalves<sup>1,2</sup> · Clara Mendoza-Martinez<sup>3</sup> · Orlando Salcedo-Puerto<sup>3</sup> · Samuel Emebu<sup>4</sup> · Eduardo Coutinho de Paula<sup>2</sup> · Marcelo Cardoso<sup>2</sup>

Received: 30 April 2024 / Accepted: 2 October 2024 / Published online: 18 October 2024  
© The Author(s) 2024

## Abstract

Pulp mill sludge is a challenging by-product in wastewater treatment plants (WWTP), due to high moisture content, and poor dewatering characteristics. Solar drying was identified as an appropriate pre-treatment to reduce sludge moisture and enhance its energy efficiency for combustion purposes. Brazil is the world's second-largest pulp producer, and its high intensity of annual solar irradiation makes it a prime candidate for the application of solar sludge drying technology. This study evaluates the main characteristics of primary sludge (PS) from pulp mills at 65% and 95% moisture content. An active passive solar dryer, followed by ASPEN Plus software simulation was used to evaluate drying properties and combustion potential. CO<sub>2</sub> emission impact was explored, and the environmental effects of primary sludge combustion after solar drying were estimated. As indicated by the findings, the sludge commenced with a solids concentration of 21%, eventually reaching 95.5%, thereby enhancing its suitability for combustion. From the simulation, a heat rate expenditure in sludge combustion reported 24672 kW and 16295 kW for a solids content of 65% and 95%, respectively. Therefore, employing solar drying before the sludge incineration is crucial for minimizing energy consumption during combustion. Additionally, solar energy being cost-free, offers an opportunity to alleviate environmental harm.

**Keywords** Active indirect solar dryer · Primary sludge · Combustion · CO<sub>2</sub> emissions · ASPEN plus software

## Introduction

Disposal of sludge generated in wastewater treatment plants (WWTPs) has been an increasing concern around the world due to environmental impact and treatment/disposal costs. Several stages and processes are often used to reduce the waste volume or reuse, to minimize the content of pollutants, and to get rid of pathogenic organisms. The correct management besides minimizing the waste volume and the toxicity,

must achieve the technical standards and satisfy current legislation [1, 2]. The most significant regulations in Europe are directives 1999/31/EEC, 2008/98/EC, 91/271/EEC, and 86/278/EEC, concerning waste landfill, urban wastewater treatment, and the use of sludge in agriculture, respectively [3]. The European Commission considered that those directives related to sludge are effective, efficient, and by other EU legislation, thus an update is not required [4].

However, upon assessing the accessible data, it is observed that sludge is utilized in agriculture in close to half of the instances, raising apprehensions regarding the potential long-term buildup of harmful elements in the soil. In South America, Brazil has encouraged studies on the use of waste and possible transformation into by-products to replace raw materials and reduce costs [5]. For industrial sludge, anaerobic and aerobic digestion, composting, chemical stabilization, drying, and soil incorporation are mainly used in Brazil for WWTP streams [6]. Currently, Brazilian Federal legislation criteria and procedures have two resolutions for the management of wastes and hazardous materials, namely: Resolution 375/2006 established by the National Council of the environment. Both resolutions outline the

✉ Clara Mendoza-Martinez  
clara.mendoza.martinez@lut.fi

<sup>1</sup> Institute of Pure and Applied Sciences, Federal University of Itajubá, Rua Irmã Ivone Drumond, 200–Industrial District II, Itabira, MG 35903-087, Brazil

<sup>2</sup> Department of Environmental Engineering, Federal University of Minas Gerais, Av. Antônio Carlos 6627, Belo Horizonte, MG 31270-901, Brazil

<sup>3</sup> School of Energy Systems, LUT University, Yliopistonkatu 34, 53850 Lappeenranta, Finland

<sup>4</sup> Department of Automatic Control and Informatics, Tomas Bata University in Zlín, Nad Stráněmi 4511, 760 05 Zlín, Czech Republic

utilization of wastewater sludge in agricultural zones, aiming to provide advantages to plantation areas while mitigating risks to human health and the environment. Additionally, Brazilian regulatory standards NR25/2011 for industrial waste, encourage waste reduction with the adoption of technological and organizational best practices [7]. The alternatives for potential uses and final disposal of the sludge can be found in Supplementary Material A.

The industrial sludges generated at WWTPs are complex mixtures of organic and inorganic compounds that may be energetically desirable or a source of problematic materials. Due to the presence of organic compounds, sludge can be used as solid fuel. Combustion is the industry's typical method to dispose of sludge in fluidized beds at over 800 °C. However, the sludge cannot be burned in autothermal mode, which requires an additional drying step. Thus, sludge is mechanically dried, reaching a percentage of solid material of 27.9% as for the case studied in this research. Furthermore, another drawback involves the introduction of detrimental substances into the exhaust gases during the incorporation of sludge into the process [8].

Diverse technologies can be applied to minimize the problems of sludge disposal, including physical (mechanical, thermal, electrical), chemical (adding oxidizer or uncoupler agent), and biological methods [9]. Recent studies have focused on performance enhancement for sludge disposal, sludge minimization, removal of contaminants, wetland sludge treatments, and residual biosolids reuse, among others [10–17]. However, independent from the process adopted, relevant limits associated with the high water

content prevent sludge energy potential from being recovered directly. Typically, sludge has a high moisture content of around 80–99% (wb) [15]. Figure 1 shows a typical representative scheme of the water removal stages of sludge.

Within moisture removal techniques, thermal drying stands out as an energy-demanding process, making solar energy a preferred and eco-friendly option due to its cost-effectiveness. Artificial dryers facilitate rapid and efficient drying through temperature control. Conversely, despite notable fluctuations in thermal conditions caused by seasonal solar availability and atmospheric variations, solar dryers exhibit considerably lower drying costs compared to artificial drying. This is attributed to the minimal direct costs associated with utilizing solar energy to heat the airflow [18, 19]. Additionally, thermal energy storage systems (TES) are effective ways to store a portion of the solar thermal energy during times of high solar radiation intensity and recover it during times of low solar radiation and night, allowing the drying process to continue. As a result, solar dryers can operate better at low cost, as the thermal storage materials are inexpensive and simple to collect. Review of different types of solar thermal dryers can be found in Supplementary Material B.

After drying, sludge combustion is typically implemented in industry since presents a major energy security and climate change mitigation options. Some developed nations promoted the conversion of solid waste into electricity to prevent environmental damage caused by waste accumulation with combustion processes. The co-combustion of sludge is an option for its energy recovery. A bubbling

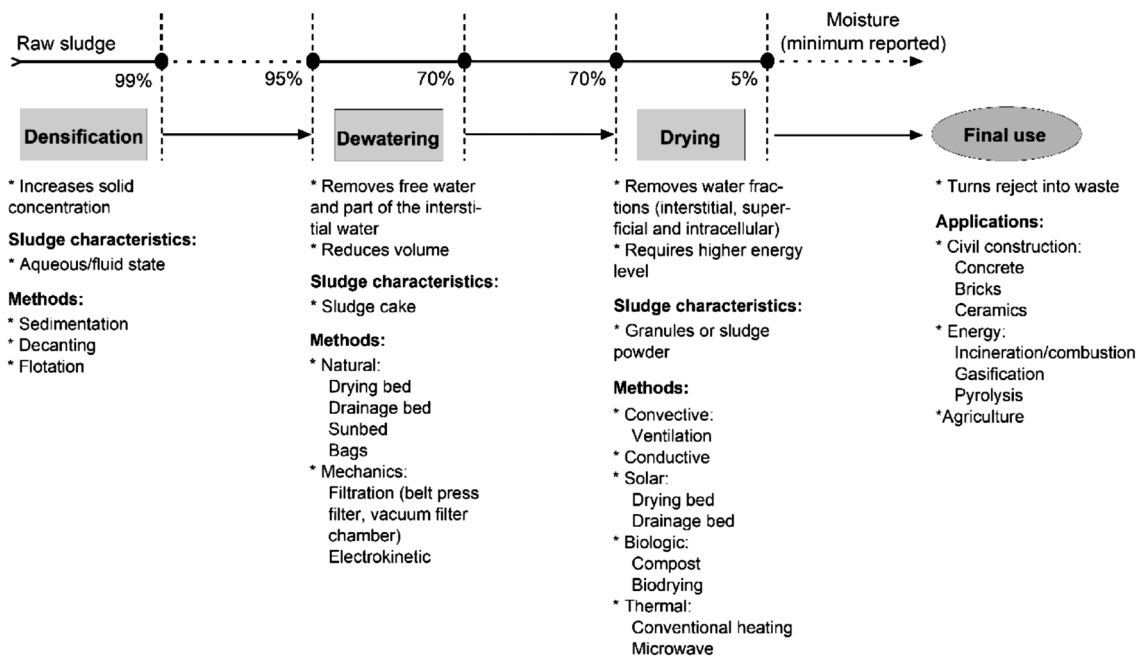


Fig. 1 Scheme of sludge treatment stages for water removal

fluidized bed reactor was built on a pilot scale at the University of Portugal campus. The main point that was studied was the emissions of gases in the exhaust, Na and Cl. Continuous monitoring related to temperature and gas composition showed that the reactor was in steady state operation. Due to the percentage of inorganic contents, ash can form and damage the equipment [8]. In Colombia, the company Smurfit Kappa generates around 320 tons/day of primary sludge in the WWTP with a solid material content of 12%. After a pre-mechanical drying treatment, it undergoes the following thermal drying technologies: incineration, co-combustion, and alternative co-processing routes, such as gasification and pyrolysis. Reducing drying costs can be achieved by mixing boiler ash, wood waste and primary sludge. And subsequently, through the pelletization process, it is possible to reduce the total mass by up to 45%, making it possible to use it for energy purposes [20].

There are three sets of reactions that can be used to model sludge combustion. These three zones have endothermic reactions, while the combustion zone's exothermic reactions provide the necessary heat. The biomass is heated in the drying zone to drive out its moisture. Then, it undergoes to the first set of reactions, which includes the decomposition process, carried out in the pyrolysis zone according to Eq. (1).



where volatile organic compounds (VOC). The second set of the byproducts of the breakdown process react on the combustion zone carried out in the pyrolysis zone according to Eqs. (2), (3) and (4).



Finally, the products of the decomposition and the combustion medium interact in the reduction zone according to the Eqs. (5), (6), (7), (8) and (9):



It is well-recognized that one of the most useful techniques for analyzing and improving a chemical process is

mathematical simulation. Modeling different chemical processes can be effectively done using ASPEN Plus®. A co-gasification approach to energy production with pulp mill sludge was simulated in ASPEN Plus software. A model was created to simulate the synergistic effects of co-gasification of the waste in question. The initial model was created using the literature and later validated with experimental data. The results achieved were 850°C temperature at 1 bar pressure, the model provided information for large-scale gasifier projects, in addition to the optimization of mixtures of different types of biomass [23]. Simulation with ASPEN Plus software of sludge combustion with a productivity of 6 tons per hour demonstrated that catalytic combustion technology can be used for mechanically dewatered sludge with a moisture content of ~75% in auto thermal mode (without the use of additional fuel). The amount of thermal energy possible to obtain can reach 3.07 MW, humidity directly affects the heating value [24]. A drying and pyrolysis process of municipal sewage sludge was simulated using ASPEN software, to propose a self-sustainable disposal of the waste. Using simulation, it was proven that the process is viable from the point of view of energy self-balance. Other points analyzed were that humidity has an impact on the system's energy consumption [25]. The technology of combustion of pulp mill sludge after the solar drying process has not been significantly reported in the literature.

In this work, a study case of solar drying was applied to primary sludge from pulp mill WWTP located in the northeast region of Brazil, using an active indirect solar dryer. The main objective of this work is to use the prototype of an active indirect solar dryer already built and installed in Belo Horizonte, Brazil, to investigate the performance of the system and optimize the design parameters [19]. The characterization of primary sludge from the cellulosic pulp industry was analyzed, and the thermal efficiency and sludge drying efficiency were calculated. Likewise, the reduction of environmental impacts was addressed, promoting drying with solar energy, analyzing the proportion of fuel and water vapor during the combustion process after drying with the ASPEN Plus software. The originality of this research lies in examining the environmental consequences starting from the solar drying of the sludge and extending to its combustion in a boiler [26]. The study aims to pinpoint the primary impacts that require attention throughout this process.

### Pulp mill sludge

Kraft plants produce, on average, 58 kg of sludge per ton of air-dried pulp ( $\text{kg tsa}^{-1}$ ) 70% refer to primary sludge and 30% to secondary sludge, in a process that uses sulphite and deinking sludge production is approximately 102 and 234 kg, respectively. The primary and secondary sludge is classified as Class II-A, it is non-hazardous and non-inert. In

2022, Brazil produced around 25 million tons of cellulose, consolidating itself as the second largest producer in the world, with eucalyptus and pine wood being the main raw materials used [2, 27–33].

Sludge is produced from the clarification process of the pulp mill wastewater stream. The sludges are primarily composed of high-fibrous organic contents such as lignin and short-chain cellulose fibers that are not suitable for pulp production. The clarification of this waste stream can be divided into primary (chemical) and secondary (biological) waste treatment, in which the by-product streams are classified as primary and secondary sludges, respectively (Fig. 2). After primary sludge separation the wastewater can undergo biological and physicochemical treatments to produce a more processed waste material known as secondary sludge; however, this study case focuses on primary sludge generated from the initial clarification stage in the pulp mill WWTP. Primary clarification leads to the production of primary sludge, which can be achieved by either sedimentation or flotation [34–38].

## Materials and methods

### Primary sludge sampling and characterization

Primary sludge was collected from a WWTP of a pulp mill located in northeastern Brazil. A representative sample of the WWTP was collected after the belt filter presses

dewatering stage in the pulp mill. The samples were packed into sealed plastic bags, then placed in Styrofoam boxes.

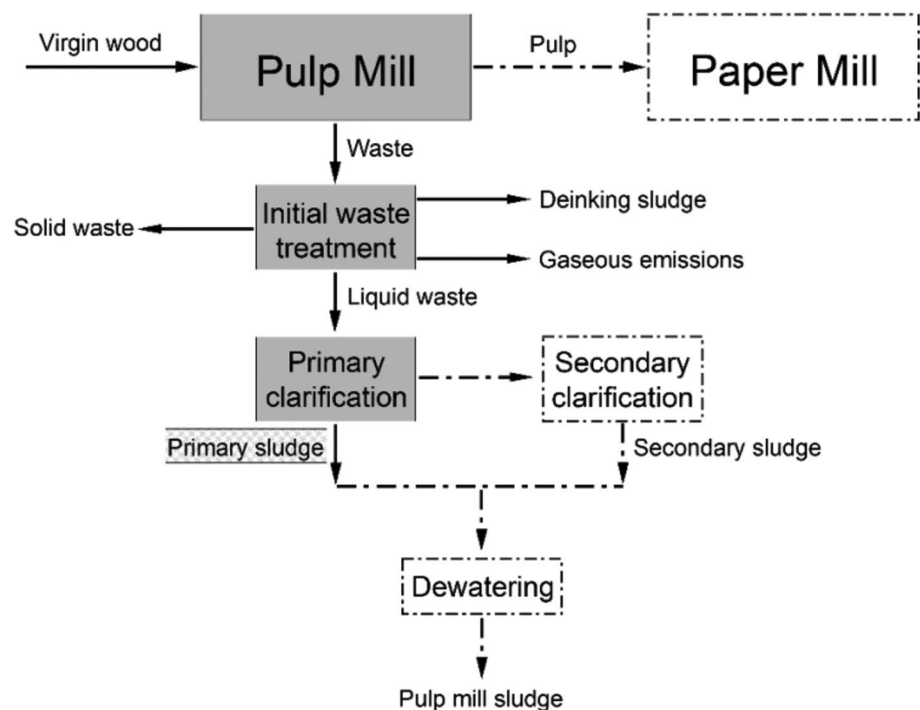
The moisture content (MC), volatile matter (VM) and ash content (AC) analysis were determined following the ISO 18123 (ISO—International Organization for Standardization., 2023a) and ISO 18222 (ISO—International Organization for Standardization., 2023b), respectively. Fixed carbon (FC) was calculated according to the following Eq. (10):

$$FC[wt\%] = 100 - (AC[wt\%] + VM[wt\%]) \quad (10)$$

The HHV was measured with a Parr 6400 bomb calorimeter according to ISO 18125. Ultimate analysis was performed using a TruSpec Micro—LECO CHN628 Series Elemental Determinator coupled with a 628S Sulphur Add-On Module according to the ISO 16948 (SFS, 2015) and ISO 16994 standard procedures. The oxygen content was approximated as the difference between 100% and the weight percentages of the major elements on a dry basis [39].

The morphology of the samples was examined by Scanning Electron Microscopy (SEM) using a Hitachi SU3500 microscope. Elemental composition of the primary sludge sample and bound metals were determined with EDS analysis using ZEISS/Gemini SEM 300 with a Bruker X-Flash 100 detector. The thermal decomposition of primary sludge was analyzed using thermogravimetric analysis (TGA) and differential thermal analysis (DTGA), carried out under oxidative atmospheres at 10 °C/min, using SHIMADZU DRG-60H system.

**Fig. 2** Primary and secondary sludge production routes from pulp mill. Modified from Turner et al. 2022 [34]



## Solar drying treatment

Tests with the active indirect solar dryer were carried out in August 2022, in 6 h of tests (10 am–4 pm), Brazilian time, Federal District, Brazil (GTM-3). The tests were performed at the beginning of winter, being the period of low relative humidity and little presence of clouds in the region [19]. The system was placed in an open area far from communities. Primary sludge has sulfurous and ammoniacal smells, that can impact the nearby community's well-being. Thus, effective odor control measures are essential to mitigate its effects. Typically, WWTP uses technologies such as biofilters, activated carbon filter, chemical treatments, dilution with other materials (e.g., wood chips) for odor control of sludge. In this study, the location provides proper ventilation, and no other odor control was needed.

The drying process with the solar dryer was divided into two stages: (i) the preheating of the air using an absorber plate with channels to increase the residence time of the air (baffle) and forced convection using a mini fan. And (ii) the drying stage of sludge in an indirect drying chamber with four compartments.

The equipment's wooden framework is covered by tempered glass measuring 8 mm in thickness, and it is externally shielded by galvanized steel sheets featuring ceramic fiber insulation. To enhance solar radiation absorption, the dryer's structure is painted in a matte black. The dryer includes a drying tray with a surface area of 0.108 m<sup>2</sup> (0.45 m × 0.24 m). With an approximate drying capacity of 2 kg of wet product per 0.108 m<sup>2</sup> of drying area, the suggested dryer's maximum drying capacity is stated as 1.98 kg [40]. Airflow is carried out by forced convection through a fan at the inlet with a maximum speed of 1.8 m/s.

The glass cover allows the passage of solar radiation, which is absorbed by the plate located inside the equipment. The heat from the airflow eliminates moisture from the product, exiting the dryer through a rectangular section containing a drying basket equipped with 4 trays on screens measuring less than 45 μm (270 mm × 230 mm) (Duffie and Beckman, 2006; Easa et al. 2024). Product insertion and extraction occur through a side door in the drying chamber. The dryer equipment is set at a 30° incline facing north. The inclination angle was determined as the absolute value of the geographical latitude, aiming to optimize the drying efficiency. In this study, TES was not included in the dryer system configuration, as solar radiation intensity during the test was high.

The temperature was measured at six points: input, output, ambient and at three selected points in the baffle with PT-100 sensors. Temperature measurements allow the analyse of temperature gain and provides data to register the availability of solar radiation incident on the device. The ambient temperature variation reported the environmental conditions.

Relative humidity of the air and dew point were measured by two thermo-hygrometers positioned at the inlet and outlet of the equipment. A pyranometer was positioned in the equipment surface to measure the available radiation, this data complements the calculations of thermal and instantaneous efficiency of the drying process. A multifunction anemometer was positioned at the entrance of the dryer to measure the air velocity provided by the fan. A data logger was in a properly shaded and ventilated shelter to record data every second of the device and ambient conditions. A router was responsible for transferring data from the data logger to the LabVIEW software. The software is used to interface the data logger with the computer, in addition to generating the graphs and assisting in the processing and conversion of data. The developed small-scale active indirect solar dryer and instrumentation positioning are presented in Fig. 3. More detailed information on the structure and dimensions of the solar dryer can be found in supplementary material C.

The uncertainty analysis was performed by the method of comparison, performing the measurement at absolute zero and at the maximum temperature of the PT-100, finding the systemic error, that is, if there is no variation between the minimum value and the maximum value, it is considered the variation value for all intermediate measurement ranges. This allows the indication of the uniformity of the wires and the reproducibility of the calibration. Equation (11) was used to calculate the thermal efficiency of the dryer ( $\eta_T$ [%]) [41].

$$\eta_T[\%] = \frac{\dot{m} \left[ \frac{\text{kg}}{\text{s}} \right] \left( h_m \left[ \frac{\text{J}}{\text{kg}} \right] - h_{out} \left[ \frac{\text{J}}{\text{kg}} \right] \right)}{A[m^2] \cdot G[W/m^2]} \quad (11)$$

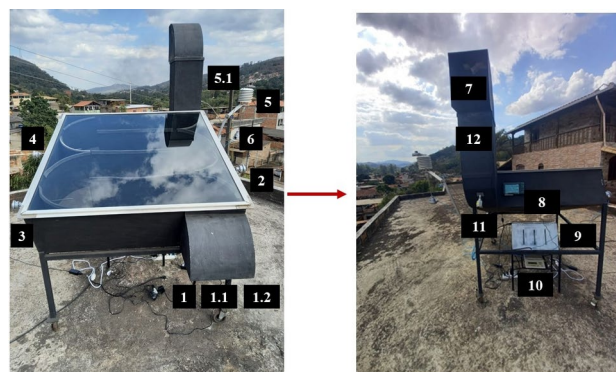


**Fig. 3** Active indirect solar dryer. 1-input temperature (TP-01), 1.1-thermal hygrometer, 1.2-multifunction anemometer, 2-center channel temperature (TP-02), 3-input channel temperature (TP-03), 4-output channel temperature (TP-04), 5-pyranometer, 5.1-shelter, 6-room temperature (TP-05), 7-temperature hygrometer sensor, 8-thermal hygrometer, 9-box with datalogger, 10-precision balance, 11-outlet temperature (TP-06), 12-chamber drying

where  $\dot{m}$  [kg/s] represents the air mass flow,  $h_{in}$  [J/kg] and  $h_{out}$  [J/kg] denote the specific enthalpies at the dryer's inlet and outlet, respectively.  $A$  [ $m^2$ ] stand for the collector area, and  $G$  [ $W/m^2$ ] represents the hemispherical solar radiation area in the collector plane.

Four sludge samples of 500 g were placed in identified trays of the drying chamber. Samples were weighed every 30 min during the tests. For each measurement data was collected three times. Essential parameters for proper solar dryer efficiency calculations, were measured, such as temperature, relative humidity and air speed at the inlet and outlet, and solar radiation incident on the plane of the device. Certified and properly calibrated equipment, in addition to statistical calculations to reduce the standard error, were used.

Drying efficiency ( $\eta_s$  [%]) was calculated by the ratio between the vaporization energy of the product water and the energy spent by the dryer [40], following Eq. (12).

$$\eta_s[\%] = \frac{\int \dot{m}_{H_2O} \left[ \frac{kg}{s} \right] \cdot h_{lv} \left[ \frac{J}{kg} \right] \cdot dt}{\int A \left[ m^2 \right] G \left[ W/m^2 \right] \cdot dt} \quad (12)$$

where  $\dot{m}_{H_2O}$  represents the instantaneous moisture flow that is withdrawn from the product in the dryer,  $h_{lv}$  denote the latent heat of vaporization. The data was critically analyzed to generate graphs that made it possible to diagnose the ideal operating conditions for the future development of new technically and environmentally viable dryer designs.

## Simulation of combustion assessment

This work presents a model of a combustion reactor based on the equilibrium model approach implemented in ASPEN Plus V11. The development of the model involves the following steps: definition of the process flowsheet, description of the stream class, selection of the property approach, and the identification of conventional and non-conventional components. Prior to providing the fuel to the reactor, the fuel was dried to reach 65% a 95% DS, simulating the solar drying stage. Pyrolysis stage follows the drying, in which the raw material is broken down into volatile chemicals and char, then the combustion occurs producing syngas.

The model's fundamental assumption:

- Process under steady state.
- No pressure drop and no heat loss are considered.
- All considered components are in chemical equilibrium.
- To reduce the hydrodynamics complexity the influence of tar and other heavy products are not considered.
- All sulfur is converted to  $H_2S$ .

Utilizing the Stoichiometric Reactor (RStoich), Yield Reactor (Ryield), and RGibbs Reactor as the major reactor types, the combustion process simulation model was developed using ASPEN Plus V11 software. Table 1 describes the models of ASPEN Plus unit operation. The simulation model is generated based on the proximate and ultimate analyses. In ASPEN Plus, PS (primary sludge) and ashes are designated as non-conventional components. HCOALGEN and DCOALIGT serve as the enthalpy and density models for these non-conventional components (PS and ash).

To simulate the drying process the 'RStoic' block was used. During this stage evaporation is used to reduce the moisture content of the feedstock. In ASPEN, all non-conventional elements have a weight of 1. The amount of materials produced on average is directly proportional to the carbon content and ash concentrations that are determined with proximate analysis. Similarly, the total production of volatiles is equal to the content of the fuel.

In the combustion stage, PS undergo a heating process, at temperatures ranging from 100 to 150 °C. This causes the particles to dry up and release moisture in the form of steam. Following the drying stage an unconventional feed consisting of dry PS goes through a breakdown process model called Ryield block, which converts the PS sample into conventional compounds such, as Carbon monoxide (CO), carbon dioxide (CO<sub>2</sub>), Hydrogen (H<sub>2</sub>), methane (CH<sub>4</sub>), Ammonia (NH<sub>3</sub>), hydrogen sulfide (H<sub>2</sub>S), water (H<sub>2</sub>O). After breakdown, the transformed elements are combusted with an air stream as a medium. This combustion stage is simulated using the accurate RGibbs reactor model, which measures chemical and phase equilibrium by reducing the system's Gibbs free energy. When all of the sulfur in the feedstock interacts with H<sub>2</sub>, H<sub>2</sub>S is created. The differences caused by this simplification are hardly noticeable due to the low sulphur level of fuel. Figure 4 shows the ASPEN Plus simulation of the solar drying process until combustion in a biomass boiler with a sludge solid material content of 65% and

**Table 1** ASPEN Plus unit operation used in this study

ASPEN Plus unit	ID of the block	Description
RStoic	Drier	Simulate the drying stage. Reduce the fuel's moisture content
RYield	Decomp	Convert non-conventional sludge into conventional components
RGibbs	Combust	Operates with three-phase equilibrium and estimates synthesis gas mixture
Sep		Split fractions. Remove water from sludge and gases from ash

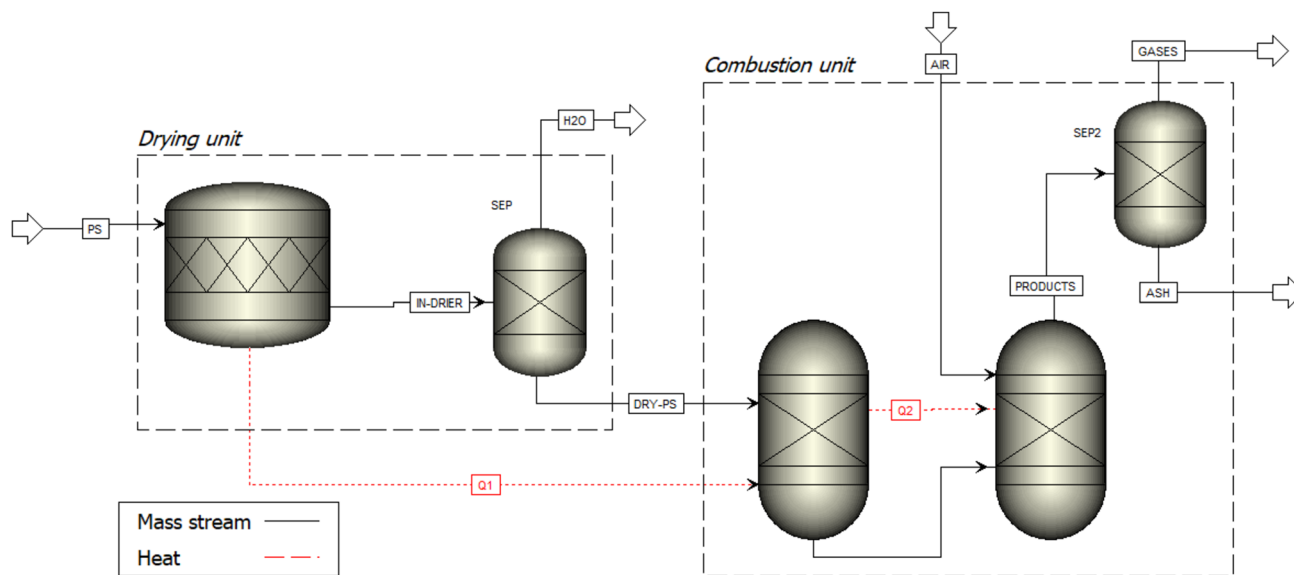


Fig. 4 Simulation of the process flow of primary sludge combustion

Table 2 Combustion process operating parameters

Parameter	Unit	Value
Feed rate	Kg/h	1000*
Feed temperature	°C	25
Feed pressure	atm	1
Air pressure	atm	1
Air temperature	°C	25
Air excess	%	15
Combustor temperature	°C	800
Combustor pressure	atm	1

\*dry basis

95% of dry solids. The base feed rate for the simulation was 1 ton of primary sludge dry basis for both scenarios (Fig. 4). Table 2 it presents combustion process operating parameters.

## Results and discussion

### Primary sludge characterization

The proximate and elemental composition analyses along with the heating values of the sludge are listed in Table 3.

Proximate analysis involves the quantification of moisture content (MC), volatile matter (VM), fixed carbon (FC) and ash content (AC). As mentioned in previous sections, MC refers to the water content in the biomass sample. High values of MC negatively affect factor such as combustion efficiency and specific heat. The studied primary sludge has a high MC of 97,02 wt% (wb), which is a typical value for

Table 3 Chemical composition of the primary sludge

Property	Primary sludge
Proximate analysis	
Moisture [wt%]	97.02
Volatiles [wt%] <sup>a</sup>	65.98
Ash [wt%] <sup>a</sup>	22.01
Fixed carbon [wt%] <sup>a</sup>	12.01
Ultimate analysis <sup>a</sup>	
Carbon [wt%]	41.64
Hydrogen [wt%]	6.3
Nitrogen [wt%]	0.67
Sulphur [wt%]	0.42
Oxygen [wt%]	28.97
Fuel ratio <sup>a</sup>	
FC/VM	0.18
Heating values <sup>a</sup>	
HHV [MJ/kg]	18.66
LHV [MJ/kg]	17.29

<sup>a</sup>Dry basis

FC fixed carbon, VM volatile matter, HHV high heating value, LHV low heating value

this type of biomass and is consistent with values previously reported (Martinez et al., 2021). This high value signifies a substantial water content within the sludge, which poses challenges during handling, transportation, and storage, as it requires intensive drying methods, increasing energy costs.

Biomass volatile are compounds that easily turn into gases when burned or decomposed. These volatiles include hydrocarbons, hydrogen, oxygen, carbon monoxide, and

some non-combustible gases (NCG). The amount of VM in a solid fuel influences factors such as ignition, flame stability, reactivity and char exhaustion [42]. The substantial volatile content (65,98 wt%) indicates that the sludge is highly susceptible to thermal degradation which means that a significant portion of the sludge can be readily vaporized or combusted when exposed to heat, indicating that it is a good source of combustible material. This means that primary sludge could be used as a fuel source, although it is important to note that primary sludge may contain harmful contaminants such as heavy metals.

Fixed carbon represents the solid carbon remaining in the char of biomass after pyrolysis and devolatilization. In simpler terms, FC indicates how much matter turns into charcoal during combustion. On the other hand, AC reveals the amount of non-combustible inorganic matter and minerals. The amount of ash in the sludge (22,01 wt%) is significantly higher compared to coal and lignocellulosic biomass, this value being between 10.28 and 31.50 wt% and 0.70–6.30 wt% respectively. Conversely, the fixed carbon content (12,01 wt%) exhibits an opposite trend, being this typically between 16.40 and 45.32 wt% for coal, and between 13.91 and 19.75 wt% for lignocellulosic biomass (Hu et al., 2022). It is worth of mention that since primary sludge contains a significant amount of inorganic components, the oxidation of inorganic elements may cause an underestimating of the fixed carbon value and an overestimation of ash content as indicated by [43]. AC stands as a prominent fuel characteristic that significantly impacts and poses challenges in the design of boilers and combustors. A number of problems such as agglomeration, fouling, erosion, corrosion, alkali-induced slagging, and sintering (in fluidized beds), can arise from elevated AC levels [44, 45].

The ultimate analysis involves determining the proportions of key elements that constitute biomass, specifically carbon (C), hydrogen (H), nitrogen (N), sulphur (S), and oxygen (O). Knowing the percentages of the main elements that constitute biomass (the concentration of carbon and hydrogen being the elements that contribute the most to the heating value of fuel), it is possible to calculate the higher heating value (HHV) or the lower heating value (LHV) of biomass (Chun-Yang Yin, 2011). Based on the ultimate analysis for the primary sludge sample, C was the dominant element measured at 41.64 wt% followed by O at 28.98 wt%, H at 6.3 wt%, N at 0.67 wt% and S at 0.42 wt% according to the weight% in db. The high contents of carbon and hydrogen suggest the existence of a significant amount of organic material, most likely due to the presence of organic fibrous material [15]. Nitrogen and sulphur contents are important parameters in the evaluation of biomass as a possible fuel use due to its harmful and corrosive potential. The low content of N and S in the studied primary sludge indicates the viability of this biomass to be used in thermochemical processes

such as combustion having low emissions of nitrogen and sulphur pollutants (Casco et al., 2023). The formation of harmful pollutants like sulphur oxides (SO<sub>x</sub>, primarily as SO<sub>2</sub>), nitrogen oxides (NO<sub>x</sub>), and other sulphide-based pollutants like carbonyl sulphide (COS) and hydrogen sulphide (H<sub>2</sub>S) can be facilitated by high concentrations of nitrogen and sulphur compounds in biomass [46]. Higher Heating Value (HHV) and Lower Heating Value (LHV) sludge were shown on a dry basis (db).

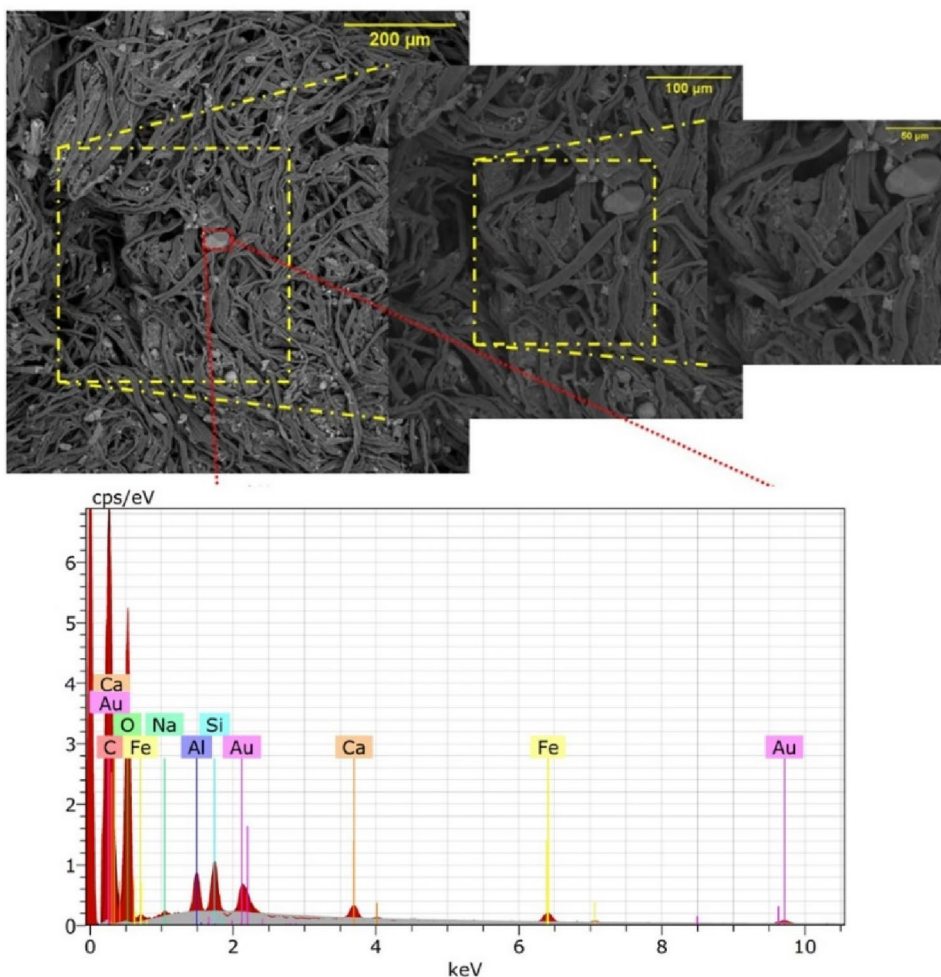
The heating value serves as an indicator of the utmost energy potential that can potentially be derived from a biomass source and is regarded as a crucial parameter for evaluating and modelling energy in thermochemical conversion processes. Nonetheless, the amount of biomass energy that can be harnessed depends on the efficiency and requirements of the conversion technology in use. The heating values of the studied primary sludge are comparable to those of other biomass, such as lignocellulosic biomass and agricultural residues [47], but lower compared to other wastes from water treatments such as sewage sludge or primary sludge from northern pulp mills. However, if the heating values are calculated considering the actual moisture content of the primary sludge the HHV and the LHV (ar) would be 0.55 and 0.51 MJ/kg, respectively. With such a low calorific value, it is unlikely that the primary sludge can be effectively used in the thermochemical conversion process for energy recovery (except hydrothermal carbonization). For this reason, it is of great importance to reduce the moisture content of this biomass, making it more suitable for use in combustion processes or for other energy applications.

Primary sludge SEM images and EDS analysis are shown in Fig. 5. The samples were analyzed to identify fiber characteristics and gather information on the integrity, structure, and presence of contaminants. Primary sludge exhibits a fibrous morphology that is long, smooth, and homogeneous, aligning with findings previously documented in [15]. For primary sludge originating from a Finnish pulp mill. Additionally, aggregates of mineral particles were observed. Fiber characteristics and information on the integrity, structure and contaminants presence in the samples, were identified.

On the primary sludge surface with SEM–EDS analysis large amounts of carbon (45.4%) and oxygen (34.9%) were found. In addition to these major elements, some minor elements were also detected in EDS analysis such as Na, Si, Al, Ca, Fe and Au. The peak energy of Ca was significant, and the concentration by volume of O<sub>2</sub> reached 51.0%. Al is also present in the layer structure in the form of particles. Primary sludge has lower N and P content than secondary sludge. And while pulp mill sludge C:N ratios can vary, primary sludge C:N ratios are much higher than typically observed ratios in natural soils. In the specific sample, there was no presence of S, but it is a common element that is present in the primary sludge of the WWTP of the pulp



**Fig. 5** SEM and EDS analysis of primary sludge from the pulp mill



industries. Probably, S volatilized during the wood delignification process during the cellulosic pulp mill process [48].

Thermogravimetric analysis (TG) in the oxidative atmosphere and its derivative (DTG) are used to determine the combustion characteristics of the primary sludge, Fig. 6. The TG curve of primary sludge combustion present continuous mass loss, taking place in stages. These three stages are: dehydration, oxidative pyrolysis, and char oxidation. In the present study, the sample subjected to thermogravimetric analysis was not previously dry, reason why the TG curve shows the primary sludge has already lost about 80% of its weight at about 150 °C, thus indicating its high moisture content. After this dehydration stage, the decomposition of volatile matter begins followed by oxidation; in the case of an oxidative atmosphere, combustion and devolatilization might happen simultaneously [21].

Devolatilization and oxidative pyrolysis corresponds mainly to the thermal degradation of the cellulose and of lignin in smaller proportions; the components degrade in different temperature ranges depending on their thermal stability. The TG curve obtained for PS show a weight decay

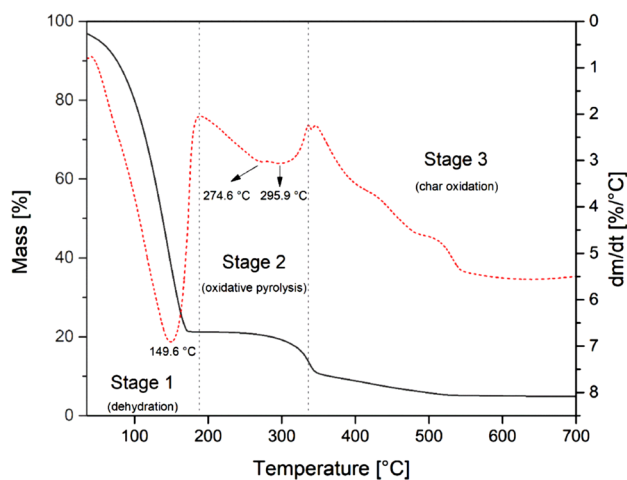


**Fig. 6** Thermal behavior of primary sludge by TGA and DTA

with a maximum in DTG in this second stage at c.a. 300 °C, which is generally assigned to cellulose decomposition [49]. In studies in which the PS was previously dried, this stage

reflects the greatest weight change and the greatest rate of mass change, this due to the rapid degradation of the volatiles that are generally the main constituent of this particular biomass [21]. In the third thermal stage, the lignin continues its decomposition without shown any characteristic peaks. However, an additional slight shoulder at 550 °C associated with charcoal combustion can be observed. The different degradation stages occurred at relatively lower temperatures, probably due to rapid reactions of volatiles at particle surface, which increases particle temperature [50].

## Solar drying test

Solar radiation, in the form of solar thermal energy is an alternative source for sludge moisture content reduction. Brazil has a high intensity solar radiation and long sunshine duration, due to the country's close location to the equator. The northeast region reported the highest levels of global irradiance, with daily averages above 5000 Wh/m<sup>2</sup> day while the lowest values of irradiance were found in the southern and northern regions of the country. Moreover, Brazil has little variation in sun incidence throughout the seasons, due to the characteristics of the earth's translation. According to the Brazilian Atlas of Solar Energy, the country receives

over 3 thousand hours of sunlight annually, corresponding to a daily solar exposure ranging from approximately 4.500 to 6.300 Wh/m<sup>2</sup> day. In the EU, Germany is a reference country for solar energy use, which receives approximately 40% less sunlight in its region of greatest sun potential, compared to the Brazilian incidence.

Figure 7A shows the influence of incident global solar radiation on the thermal parameters of the runoff generated by the dryer. Figure 7B shows the flow behavior of the solar dryer, by means mass flow curves. Figure 7C shows the drying curve performed on a particular day with partially cloudy skies. The instantaneous moisture content of the product is on a wet basis as a function of solar time. Figure 7D shows the thermal efficiency of the solar dryer with load. The variation of the instantaneous thermal efficiency for the test days was from 8.1 to 25.2%.

Global solar radiation cannot maintain constancy, this is due to the presence of clouds. In one of the curves a greater variation was observed due to the mentioned phenomena (Fig. 7A). The behavior of the air can be explained by the reduction in density due to the increase in temperature inside the equipment (Fig. 7B, D) As can be seen, the calculated instantaneous thermal efficiency of the dryer increased around noon, which is contrary to what was expected, since

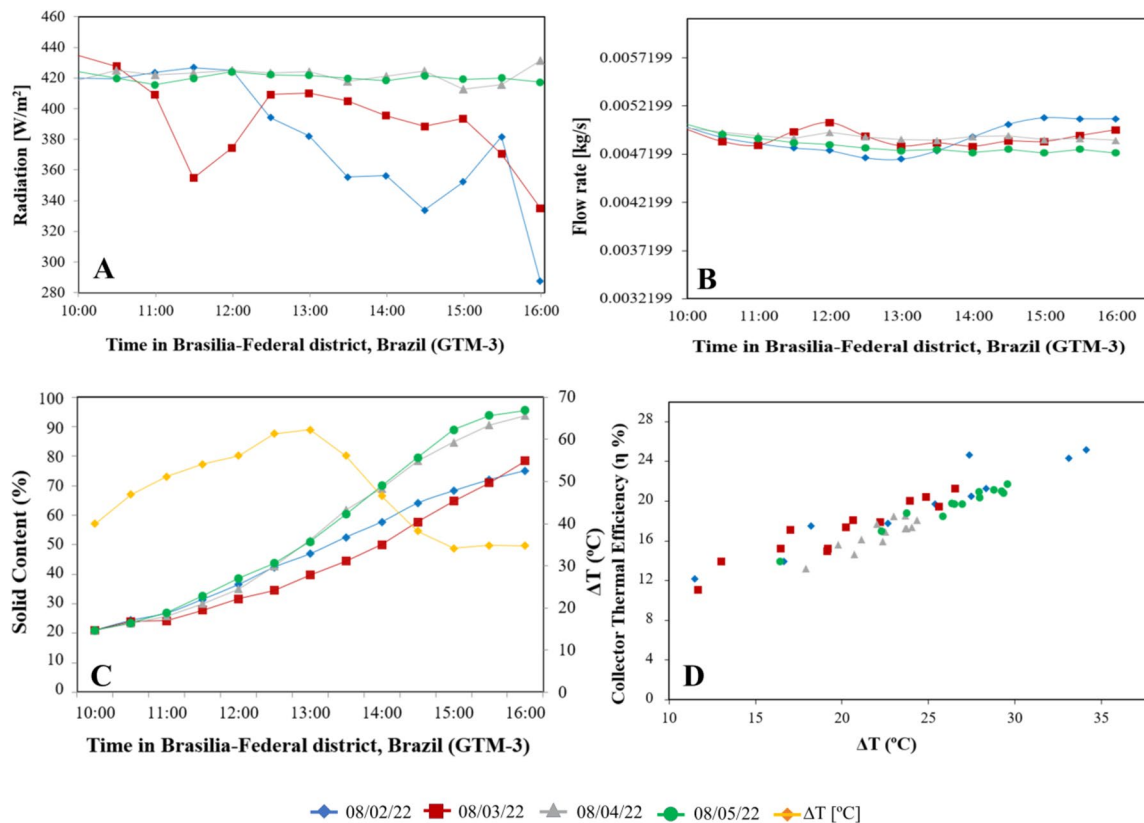


**Fig. 7** Solar drying tests of primary sludge from the pulp industry in Brazil: **A** hemispherical solar radiation in the dryer plane, **B** flow mass flow rate, **C** drying curve and **D** thermal efficiency

that it is expected that with the increase of the internal temperature of the air in the dryer in relation to the ambient temperature should promote the increase of thermal losses by the carcass of the dryer. As depicted in Fig. 7C, it is observable that in the initial testing hours, the drying curve exhibits a more pronounced attenuation, indicating a more substantial removal of surface water from the residue in accordance with drying standards [51].

The average radiation incident on the device was around  $(287.4 \pm 1.0) \text{ W/m}^2$  and  $(434.7 \pm 1.0) \text{ W/m}^2$  with an average of  $404.1 \text{ W/m}^2$  and the average  $\Delta T$  was  $(34.1 \pm 0.6) ^\circ\text{C}$  and  $(62.2 \pm 0.6) ^\circ\text{C}$  with an average temperature of  $34.1 ^\circ\text{C}$ . The instantaneous thermal efficiency of the solar dryer without a load fluctuated between 17.6% and 25.2% during the test conducted under varying climatic conditions. The efficiency was 21.0% of the initial solid mass, ultimately reaching 95.5% of the solid mass by the conclusion of the tests.

### Combustion simulation results

Samples with lower moisture content have a higher probability of undergoing a homogeneous ignition and combustion mode. Combustion with low moisture content involves a two-stage process, encompassing volatile combustion and char combustion. Conversely, samples with high moisture content undergo simultaneous gas-phase volatile combustion and heterogeneous combustion. Elevated moisture content enhances carbon oxidation, linked to the augmentation of pore surface area and the presence of oxygen atoms during moisture evaporation. The liberation of moisture and volatile matter enhances buoyancy and diminishes the convective intensity of sludge particles. Concurrently, the reaction between char and moisture amplifies the release of  $\text{CO}_2$  and  $\text{H}_2$ . Consequently, volatile matter can combust within a short distance. Additionally, moisture may contribute to an increase in oxygen-containing functional groups and oxygen atoms [22, 52].

Typically, the presence of moisture during particle combustion results in the fragmentation of the samples, whereas dry particles exhibit greater resistance to breaking. Consequently, elevated moisture contents are observed to increase the likelihood of fragmentation. A slight difference in gas production was observed, mainly due to the vapor produced caused by the moisture released. A difference of about 200 kg/hr from 65% DS to 95% DS was reported. Moreover, as the dry solid (DS) content rises from 65 to 95%, there is a decrease in  $\text{CO}_2$  emissions from 7851.57 kg/h to 4758.61 kg/h. This can be attributed to sludge biogenic nature, and to combustion efficiency. Because higher levels of DS lead to better combustion conditions, resulting in more complete oxidation of organic matter, thus reducing the release of unburned carbon compounds, including  $\text{CO}_2$ . The decrease in  $\text{CO}_2$  emissions also underscores the

impact of humidity on combustion and the subsequent escalation in environmental consequences. The increase in solids content from 65 to 95% during the drying process reduced energy consumption during the sludge combustion process in a biomass boiler from 24.67 to 16.30 kW. This signifies a decrease of around 34% in energy consumption during the sludge incineration process. Consider the potential contribution of employing solar drying for waste, not only resulting in a diminished environmental footprint but also being a low-cost alternative [53, 54].

### Conclusion

The case studied demonstrates the importance of using renewable energy for a drying process. According to the results, it can be observed that the process variables are linked to the physical characteristics of the equipment, as well as to the environmental conditions at the time of the tests. The process parameters were presented with the dryer without load, to know the thermal efficiency of the equipment. This calculation enables the assessment of the equipment's capacity to heat the air, as lower air humidity enhances its effectiveness in extracting moisture from the waste. In the drying trials involving the primary sludge from the pulp industry using the solar dryer, it was noted that a solid material proportion ranging from 21.0 to 95.5% was achieved after six hours of drying. This outcome would be advantageous if the intention is to incinerate the sludge in a biomass boiler.

Moreover, the technical viability of the solar dryer is evident as it successfully dried primary sludge from the pulp mill, reducing its relative humidity by as much as 27.8% within a 6-h testing period. According to the ASPEN model,  $\text{CO}_2$  emissions were determined to be 7345.97 kg/h for a solids content of 65% and 4758.59 kg/h for a solids content of 95%. Another noteworthy aspect concerning the utilization of solar energy for waste drying involves the advancement of technologies capable of storing heat absorbed from solar radiation. This becomes crucial for enhancing the efficiency of solar dryers, ensuring that all absorbed thermal energy is utilized optimally during periods when solar radiation is unavailable.

The variability of the instantaneous thermal efficiency was between 17.6 and 25.2%. Hence, the need to develop a hybrid solar dryer that works in an autonomous regime (off-grid) was realized with the supply of electrical energy to the fan located at the entrance of the device, which is responsible for forced convection. The increase in solids content from 65 to 95% during the drying process reduced energy consumption during the sludge combustion process in a biomass boiler from 24.67 to 16.30 kW. This represents a reduction of approximately 34% in energy consumption in

the sludge-burning process. Consider the potential contribution of employing solar drying for waste, not only resulting in a diminished environmental footprint but also being a low energy cost alternative. In future studies, the aim is to pre-heat the air using solar energy in the device, passing through a cross-flow mixer that will be fed by thermal energy from a heat blower that simulates process gases.

**Supplementary Information** The online version contains supplementary material available at <https://doi.org/10.1007/s10163-024-02095-2>.

**Funding** Open Access funding provided by LUT University (previously Lappeenranta University of Technology (LUT)).

## Declarations

**Conflict of interest** Authors declare no conflict of interest.

**Open Access** This article is licensed under a Creative Commons Attribution 4.0 International License, which permits use, sharing, adaptation, distribution and reproduction in any medium or format, as long as you give appropriate credit to the original author(s) and the source, provide a link to the Creative Commons licence, and indicate if changes were made. The images or other third party material in this article are included in the article's Creative Commons licence, unless indicated otherwise in a credit line to the material. If material is not included in the article's Creative Commons licence and your intended use is not permitted by statutory regulation or exceeds the permitted use, you will need to obtain permission directly from the copyright holder. To view a copy of this licence, visit <http://creativecommons.org/licenses/by/4.0/>.

## References

- Kacprzak M, Fijałkowski K, Grobelak A, Rosikoń K, Rorat A (2015) *Escherichia coli* and *salmonella* spp. Early diagnosis and seasonal monitoring in the sewage treatment process by EMA-QPCR method. *Polish J Microbiol.* 64: 143–148. <https://doi.org/10.33073/pjm-2015-021>
- ABNT (2004) ABNT NBR 10004: Resíduos Sólidos - Classificação (solid waste classification). Assoc Bras Normas Técnicas. 18: 71
- European Commission (2001) Disposal and Recycling routes for sewage sludge part 2-regulatory report; Luxembourg
- Gianico A, Braguglia CM, Gallipoli A, Montecchio D, Mininni G (2021) Land application of biosolids in Europe: possibilities, con-straints and future perspectives. *Water.* 13: 103. <https://doi.org/10.3390/W13010103>
- Sellitto MA, de Almeida FA (2020) Strategies for Value recovery from industrial waste: case studies of six industries from Brazil. *Benchmarking Int J* 27:867–885. <https://doi.org/10.1108/BIJ-03-2019-0138>
- Hamilton L, Garbossa P, Andreoli CV, Garbossa LHP, Lupatini G, Pegorini ES (2008) Wastewater sludge management: a Brazilian approach
- CONAMA Resolution 357. Defines criteria and procedures for the agricultural use of sewage sludge generated in sewage treatment plants and their derivative products, and makes other provisions
- Pio DT, Tarelho LAC, Nunes TFV, Baptista MF, Matos MAA (2020) Co-combustion of residual forest biomass and sludge in a pilot-scale bubbling fluidized bed. *J Clean Prod.* 249: 119309. <https://doi.org/10.1016/J.JCLEPRO.2019.119309>
- Xiong Q, Yang Y, Xu F, Pan Y, Zhang J, Hong K, Lorenzini G, Wang S (2017) Overview of computational fluid dynamics simulation of reactor-scale biomass pyrolysis. *ACS Sustain Chem Eng.* <https://doi.org/10.1021/acssuschemeng.6b02634>
- Ding A, Zhang R, Ngo HH, He X, Ma J, Nan J, Li G (2021) Life cycle assessment of sewage sludge treatment and disposal based on nutrient and energy recovery: a review. *Sci Total Environ* 769:144451. <https://doi.org/10.1016/J.SCITOTENV.2020.144451>
- Jafari M, Botte GG (2020) Electrochemical treatment of sewage sludge and pathogen inactivation. *J Appl Electrochem.* 51: 119–130. <https://doi.org/10.1007/S10800-020-01481-6>
- Joo SH, Monaco FD, Antmann E, Chorath P (2015) Sustainable approaches for minimizing biosolids production and maximizing reuse options in sludge management: a review. *J Environ Manag* 158:133–145. <https://doi.org/10.1016/J.JENVMAN.2015.05.014>
- Li H, Shi F, An Q, Zhai S, Wang K, Tong Y (2021) Three-dimensional hierarchical porous carbon derived from lignin for supercapacitors: insight into the hydrothermal carbonization and activation. *Int J Biol Macromol* 166:923–933. <https://doi.org/10.1016/j.ijbiomac.2020.10.249>
- Liew CS, Yunus NM, Chidi BS, Lam MK, Goh PS, Mohamad M, Sin JC, Lam SM, Lim JW, Lam SS (2022) A review on recent disposal of hazardous sewage sludge via anaerobic digestion and novel composting. *J Hazard Mater* 423:126995. <https://doi.org/10.1016/J.JHAZMAT.2021.126995>
- Mendoza MCL, Sermyagina E, Saari J, de Silva JM, Cardoso M, de Almeida MG, Vakkilainen E (2021) Hydrothermal carbonization of lignocellulosic agro-forest based biomass residues. *Biomass Bioenergy.* 147: 106004. <https://doi.org/10.1016/j.biombioe.2021.106004>
- Sharma P, Singh SP (2021) Pollutants characterization and toxicity assessment of pulp and paper industry sludge for safe environmental disposal. *Emerg Treat Technol Waste Manag.* [https://doi.org/10.1007/978-981-16-2015-7\\_10](https://doi.org/10.1007/978-981-16-2015-7_10)
- Zhao J, Hou T, Lei Z, Shimizu K, Zhang Z (2021) Performance and stability of biogas recirculation-driven anaerobic digestion system coupling with alkali addition strategy for sewage sludge treatment. *Sci Total Environ* 783:146966. <https://doi.org/10.1016/J.SCITOTENV.2021.146966>
- Di Fraia S, Figaj RD, Massarotti N, Vanoli L (2019) Corrigendum to “An integrated system for sewage sludge drying through solar energy and a combined heat and power unit fuelled by biogas” [Energy conversion and management 171 (2018) 587–603]. *Energy Convers Manag* 185:892–893. <https://doi.org/10.1016/J.ENCONMAN.2018.12.017>
- Gonçalves LM, Mendoza-Martinez C, Rocha EPA, de Paula EC, Cardoso M (2023) Solar drying of sludge from a steel-wire-drawing industry. *Energies.* 16: 6314. <https://doi.org/10.3390/EN16176314>
- Valdés CF, Marrugo GP, Chejne F, Marin-Jaramillo A, Franco-Ocampo J, Norena-Marin L (2020) Co-gasification and co-combustion of industrial solid waste mixtures and their implications on environmental emissions, as an alternative management. *Waste Manag* 101:54–65. <https://doi.org/10.1016/J.WASMAN.2019.09.037>
- Casco ME, Moreno V, Duarte M, Sapag K, Cuña A (2023) Valorization of primary sludge and biosludge from the pulp mill industry in Uruguay through hydrothermal carbonization. *Waste Biomass Valorization* 1:1–15. <https://doi.org/10.1007/S12649-023-02105-8/FIGURES/7>
- Xu J, Liao Y, Yu Z, Cai Z, Ma X, Dai M, Fang S (2018) Co-combustion of paper sludge in a 750 t/d waste incinerator and effect of sludge moisture content: a simulation study. *Fuel* 217:617–625. <https://doi.org/10.1016/J.FUEL.2017.12.118>
- Rosha P, Ibrahim H (2022) Technical feasibility of biomass and paper-mill sludge co-gasification for renewable fuel production

- using ASPEN Plus. *Energy* 258:124883. <https://doi.org/10.1016/J.ENERGY.2022.124883>
24. Fedorov AV, Dubinin YV, Yeletsky PM, Fedorov IA, Shelest SN, Yakovlev VA (2021) Combustion of sewage sludge in a fluidized bed of catalyst: ASPEN Plus model. *J Hazard Mater* 405:124196. <https://doi.org/10.1016/J.JHAZMAT.2020.124196>
  25. Zhou A, Wang X, Yu S, Deng S, Tan H, Mikulčić H (2023) Process design and optimization on self-sustaining pyrolysis and carbonization of municipal sewage sludge. *Waste Manag* 159:125–133. <https://doi.org/10.1016/J.WASMAN.2023.01.035>
  26. Chen S, Xu Y, Guo K, Yue X (2023) Rheological properties and volumetric isothermal expansivity of bamboo kraft black liquor with high solids content and low lignin content. *Sci Rep* 13:2400. <https://doi.org/10.1038/s41598-023-29350-0>
  27. Devi P, Saroha AK (2014) Risk analysis of pyrolyzed biochar made from paper mill effluent treatment plant sludge for bio-availability and eco-toxicity of heavy metals. *Bioresour Technol* 162:308–315. <https://doi.org/10.1016/j.biortech.2014.03.093>
  28. do Carmo PLA, Mudadu SC, Pereira RA, de Ávila RF (2018) Biogas production from thermophilic anaerobic digestion of kraft pulp mill sludge. *Renew Energy*. 124: 40–49. <https://doi.org/10.1016/J.RENENE.2017.08.044>
  29. Fahim S, Nisar N, Ahmad Z, Asghar Z, Said A, Atif S, Ghani N, Qureshi N, Soomro GA, Iqbal M et al (2019) Managing paper and pulp industry by-product waste utilizing sludge as a bio-fertilizer. *Polish J Environ Stud*. <https://doi.org/10.15244/pjoes/83614>
  30. Gavrilescu D (2008) Energy from biomass in pulp and paper mills. *Environ Eng Manag J* 7:537–546
  31. Gurram RN, Al-Shannag M, Lecher NJ, Duncan SM, Singasaas EL, Alkasrawi M (2015) Bioconversion of paper mill sludge to bioethanol in the presence of accelerants or hydrogen peroxide pretreatment. *Bioresour Technol* 192:529–539. <https://doi.org/10.1016/J.BIORTECH.2015.06.010>
  32. Martinez CLM, Sermiyagina E, Vakkilainen E (2021) Hydrothermal carbonization of chemical and biological pulp mill sludges. *Energies*. 14: 5693. <https://doi.org/10.3390/EN14185693>
  33. Namazi AB, Allen DG, Jia CQ (2015) Microwave-assisted pyrolysis and activation of pulp mill sludge. *Biomass Bioenerg* 73:217–224. <https://doi.org/10.1016/J.BIOMBIOE.2014.12.023>
  34. Turner T, Wheeler R, Oliver IW (2022) Evaluating land application of pulp and paper mill sludge: a review. *J Environ Manag* 317:115439. <https://doi.org/10.1016/J.JENVMAN.2022.115439>
  35. Gubelt G, Lumpe C, Verstraeten E, Joore L (2000) Towards zero liquid effluent at Niederauer Mühle: the validation of two novel separation technologies. *Pap Technol* 41:41–48
  36. Pokhrel D, Viraraghavan T (2004) Treatment of pulp and paper mill wastewater—a review. *Sci Total Environ* 333:37–58
  37. Smook GA (2002) Handbook for pulp & paper technologists
  38. Thompson G, Swain J, Kay M, Forster CF (2001) The treatment of pulp and paper mill effluent: a review. *Bioresour Technol* 77:275–286
  39. ISO - International Organization for Standardization (2017) ISO 18125:2017—solid biofuels. Determination of calorific value
  40. Leon MA, Kumar S, Bhattacharya SC (2002) A comprehensive procedure for performance evaluation of solar food dryers. *Renew Sustain Energy Rev* 6:367–393. [https://doi.org/10.1016/S1364-0321\(02\)00005-9](https://doi.org/10.1016/S1364-0321(02)00005-9)
  41. Rede Brasileira de Calibração – RBC. Available online: [http://inmetro.gov.br/laboratorios/rbc/detalhe\\_laboratorio.asp?num\\_certificado=3&situacao=AT&area=TEMPERATURAEUMI DADE](http://inmetro.gov.br/laboratorios/rbc/detalhe_laboratorio.asp?num_certificado=3&situacao=AT&area=TEMPERATURAEUMI DADE). Accessed on 11 Aug 2022
  42. Ilham Z (2021) Biomass classification and characterization for conversion to biofuels. In: Value-chain of biofuels. Fundamentals, technology, and standardization. pp. 69–87
  43. Chan WP, Wang JY (2016) Comprehensive characterisation of sewage sludge for thermochemical conversion processes—based on Singapore survey. *Waste Manag* 54:131–142. <https://doi.org/10.1016/J.WASMAN.2016.04.038>
  44. Niu Y, Tan H, Hui S (2016) Ash-related issues during biomass combustion: alkali-induced slagging, silicate melt-induced slagging (ash fusion), agglomeration, corrosion, ash utilization, and related countermeasures. *Prog Energy Combust Sci* 52:1–61
  45. Vakkilainen EK (2017) Solid biofuels and combustion. In: Steam generation from biomass. Lappeenranta, Finland. pp. 18–56. ISBN 978-0-12-804389-9
  46. Wielgoński G, Lechtańska P, Namiecińska O (2017) Emission of some pollutants from biomass combustion in comparison to hard coal combustion. *J Energy Inst* 90:787–796. <https://doi.org/10.1016/J.JOEL.2016.06.005>
  47. Marrugo G, Valdés CF, Chejne F (2016) Characterization of Colombian agroindustrial biomass residues as energy resources. *Energy Fuels* 30:8386–8398. <https://doi.org/10.1021/ACS.ENERGYFUELS.6B01596>
  48. Faubert P, Barnabé S, Bouchard S, Côté R, Villeneuve C (2016) Pulp and paper mill sludge management practices: what are the challenges to assess the impacts on greenhouse gas emissions? *108: 107–133*. <https://doi.org/10.1016/j.resconrec.2016.01.007>
  49. Yang H, Yan R, Chen H, Lee DH, Zheng C (2007) Characteristics of hemicellulose, cellulose and lignin pyrolysis. *Fuel*. <https://doi.org/10.1016/j.fuel.2006.12.013>
  50. Daouk E, Van de Steene L, Paviet F, Salvador S (2015) Thick wood particle pyrolysis in an oxidative atmosphere. *Chem Eng Sci* 126:608–615. <https://doi.org/10.1016/j.ces.2015.01.017>
  51. Duffie JA, Beckman WA (2013) Solar engineering of thermal processes. John Wiley & Sons, New York. ISBN 0470873663
  52. Horák J, Laciok V, Krpec K, Hopan F, Dej M, Kubesa P, Ryšavý J, Molchanov O, Kuboňová L (2020) Influence of the type and output of domestic hot-water boilers and wood moisture on the production of fine and ultrafine particulate matter. *Atmos Environ* 229:117437. <https://doi.org/10.1016/J.ATMOSENV.2020.117437>
  53. Price-Allison A, Mason PE, Jones JM, Barimah EK, Jose G, Brown AE, Ross AB, Williams A (2023) The impact of fuelwood moisture content on the emission of gaseous and particulate pollutants from a wood stove. *Combust Sci Technol* 195:133–152. <https://doi.org/10.1080/00102202.2021.1938559>
  54. Sepman A, Ögren Y, Wennebro J, Wiinikka H (2022) Simultaneous diagnostics of fuel moisture content and equivalence ratio during combustion of liquid and solid fuels. *Appl Energy* 324:119731. <https://doi.org/10.1016/J.APENERGY.2022.119731>

**Publisher's Note** Springer Nature remains neutral with regard to jurisdictional claims in published maps and institutional affiliations.